Evaluation of the ^{238}U Neutron Cross Section in the Unresolved Resonance Range

Arnaud Courcelle, Hervé Derrien, Luiz C. Leal, Nancy Larson

NUCLEAR SCIENCE AND ENGINEERING: **156**, 391–402 (2007)

Evaluation of the ^{238}U Neutron Cross Section in the Unresolved Resonance Range

Arnaud Courcelle*

CEA/DEN-Cadarache, 13108 Saint Paul Lez Durance, Cedex, France

and

Hervé Derrien, Luiz C. Leal, and Nancy M. Larson

Oak Ridge National Laboratory, Oak Ridge, Tennessee 37831-6171

Received May 17, 2006
Accepted September 29, 2006

Abstract—*This paper presents a new analysis of the ^{238}U cross sections in the unresolved resonance range, from 20 to 150 keV. Statistical analysis of the resonance parameters in the resolved resonance range with random-matrix theory provides accurate experimental values of strength function, average radiative width and average level spacing for s- and p-wave resonances. Above 20 keV, the simultaneous fit of selected experimental data (average transmission and capture) is performed with a statistical model of nuclear reactions as implemented in the SAMMY code.*

Compared to previous evaluations, such as those described by Fröhner or by Maslov et al., this work benefits from the accurate transmission data measured by Harvey et al. at Oak Ridge Electron Linear Accelerator, which have never been studied before. This new evaluation was written into the current ENDF format for use in practical applications. This work stresses the need for an improved ENDF format to store average resonance parameters and cross sections in the unresolved resonance range.

I. INTRODUCTION

A new evaluation of the ^{238}U neutron cross section in the unresolved resonance range, from 20 to 150 keV is described. This energy range is of importance in the neutronic calculations of both thermal and fast breeder reactors. One crucial aspect of evaluations in the unresolved resonance range is that reporting only pointwise cross sections is not sufficient: Nuclear data users require further information on resonance parameters to model resonance shielding (i.e., the drop of neutron flux in the vicinity of resonances) and temperature effects in neutron transport calculations.

The evaluation performed by Fröhner[1] 20 yr ago is considered as a reference work and is still adopted in the most recent version of JEFF and ENDF/B nuclear data libraries. The evaluation of Fröhner was carefully validated with recent capture and total measurements as well as energy-averaged transmission data through thick samples and self-indication ratios.[2]

However, several reasons justify a new investigation:

1. A recent evaluation of the ^{238}U resolved-resonance parameters has been produced by the Oak Ridge National Laboratory (ORNL) in collaboration with the Commissariat à l'Energie Atomique[3] (CEA) below 20 keV. Statistical analysis of the new set of resonances provides updated and accurate values of s- and p-wave strength functions (S_0 and S_1, respectively), average radiative widths, as well as the level density (or spacing D) at low energy.

2. The high-resolution transmission data by Harvey et al.[4] and capture data by Macklin et al.,[5] which

*E-mail: arnaud.courcelle@cea.fr

were measured up to 150 keV at the Oak Ridge Electron Linear Accelerator (ORELA) in 1988, are fully analyzed for the first time. The fluctuations in the average total and capture cross section are well measured by these experiments. These structures, likely related to the local fluctuations of the level-spacing and reduced-width distributions, are discussed briefly.

II. STATISTICAL ANALYSIS OF ^{238}U RESONANCE PARAMETERS

We have investigated the sample of s- and p-wave resonances from a recent ORNL evaluation.[3] This evaluation was based on a comprehensive experimental database from thermal energy to 20 keV. Several transmission and capture measurements, mostly performed at ORELA, were fitted with the Reich-Moore approximation of R-matrix theory using the SAMMY code.[6] Careful attention was paid to the study of experimental conditions (normalization, background, resolution function, temperature). Complementary techniques have permitted the separation between s-waves and p-waves observed resonances:

1. The theory of conditional probability gives the probability of a resonance with a given $g\Gamma_n$ to be $l = 0$ or $l = 1$ (Ref. 7). This method suggests appropriate values for the orbital angular momentum by discriminating resonances according to the magnitude of their neutron reduced widths.

2. Below 1.6 keV, Corvi et al.[8] have determined the orbital angular momentum of ^{238}U resonances by analyzing the gamma-ray spectrum following resonant capture. They noticed that the γ transitions involved in the decay of the compound nucleus are not the same in the case of s- or p-wave resonances. The γ multiplicity is enhanced for p-waves, providing a way to identify the orbital momentum.

3. S-wave resonances can be detected by the asymmetry in the transmission data due to the potential-resonant interference. More generally, the simultaneous fitting of transmission and capture measurements and the analysis of the goodness of fit permitted the assignment of l for resonances with large reduced neutron widths.

The sample of p-wave resonances contains a large number of resonances that could not be detected in the experimental data. These unseen resonances were randomly added in order to minimize the effect of the missed levels on the calculated capture cross sections. Above 10 keV, poor experimental resolution makes resonance analysis difficult so that even resonance energies could not be reliably determined. A "pseudo-resonance" approach was used; a set of resonances was proposed that fits the transmission and capture data but does not accurately represent actual resonances. Consequently, resonances above 10 keV are not studied in the present statistical analysis.

The first step is to investigate the purity of the three populations of resonances: $J^\pi = 1/2^+$, $J^\pi = 1/2^-$, and $J^\pi = 3/2^-$. For s-wave resonances, quick inspection of the plot of the cumulative number of levels versus energy (Fig. 1), as well as spacing and reduced width distribution (Fig. 2), does not permit easy determination of the proportion of missing or spurious levels.

The random matrix theory[9,10] (RMT) provides more efficient tools to analyze a sequence of resonances. The random matrix model assumes that the nuclear Hamiltonian of a compound nucleus is represented by $N \times N$ real symmetric matrices of high order, whose elements are randomly distributed and independent [the ensembles of such matrices are known as the Gaussian orthogonal ensemble (GOE)]. Statistical properties of energy levels and wave functions are deduced from the eigenvalues and eigenvectors of the random matrix. The fluctuation properties of nuclear spectra are measured by various statistics. In the present work, comparison of experimental data with GOE theory is made with Monte Carlo methods[11] (i.e., generation and diagonalization of a large number of 1500×1500 real, symmetric matrices). Various statistics on $J^\pi = 1/2^+$ levels below 5 keV were investigated.

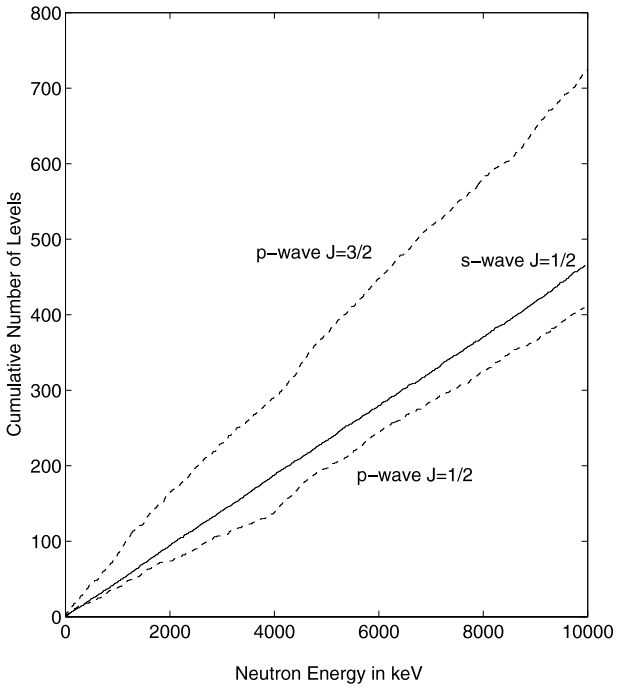

Fig. 1. Plot of cumulative number of levels for the s- (straight line) and p-wave (dashed line) resonances.

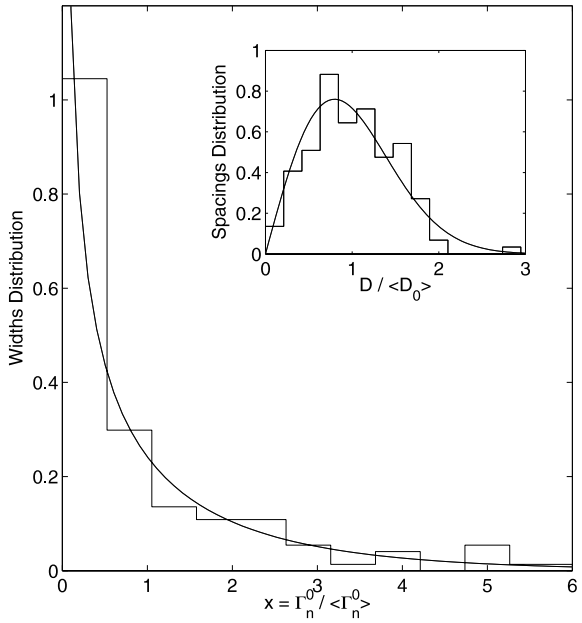

Fig. 2. Distribution of ^{238}U s-wave reduced neutron widths below 3 keV compared with a fitted truncated Porter-Thomas distribution. The small figure shows the comparison between experimental spacings distribution with the Wigner formula.

1. The fluctuation of the number of levels in an energy interval of fixed length r (in units of observed average spacing $\Delta E = r * D_{obs}$) is measured by the so-called number variance $\Sigma^2(r)$. Table I shows reasonable agreement between the $J^\pi = 1/2^+$ experimental data and GOE prediction up to 2.5 keV (and even up to 5 keV). As a more stringent test, the third and fourth moments of this number-of-levels distribution (or equivalently the skewness γ_1 and excess γ_2) were also studied; reasonable agreement was found below 2.5 keV.

2. The distribution of the nearest-neighbor spacings follows the Wigner surmise. RMT also provides theoretical forms of the spacing distribution $P(k, r)$ (and the associated spacing variance σ_k) of higher order k (i.e., the distribution of spacings between two resonances having k resonances between them). This test does not appear to be very sensitive to the presence of spurious levels, and good agreement between ^{238}U s-wave resonances and GOE prediction is again observed up to 5 keV.

3. The short-range correlations between levels are measured by the linear correlation coefficient between nearest-neighbor level spacings. A theoretical correlation $\rho(D_i, D_{i+1}) = -0.27$ is demonstrated with GOE and confirmed by the present Monte Carlo simulations. Depending on the energy range studied, the experimental correlation coefficient lies between -0.2 and -0.35, and no problem is detected below 5 keV.

4. The Δ_3 (Ref. 9) statistics is a more powerful measure of long-range correlations in nuclear spectra. It is defined as the mean square of the deviation of the cumulative number of levels (seen as a continuous function) from a fitted straight line. This test is very sensitive to the presence of impurities. As shown in Fig. 3, the agreement is fair between resonance data and theory below 3 keV. The experimental Δ_3 is overestimated at higher energies, indicating there may be missed or spurious levels (for instance, contamination of the s-wave set by p-wave resonances).

5. As discussed in Ref. 12, the F-Dyson statistic was introduced to provide a method to detect locally missed and spurious levels. For each resonance, a simple

TABLE I

Synthesis of the Statistics for ^{238}U s- and p-wave Resonances Compared with GOE Results*

Statistic	GOE Theory	Experimental ^{238}U $J^\pi = 1/2^+$ [0 to 2.5 keV]	Experimental ^{238}U $J^\pi = 1/2^-$ [0 to 2.5 keV]	Experimental ^{238}U $J^\pi = 3/2^-$ [0 to 2.5 keV]
Δ_3	0.476	0.487	0.388	8.65
ρ	−0.27	−0.32	0.09	−0.02
$\Sigma^2(1)$	0.44	0.45	0.56	0.70
$\Sigma^2(3)$	0.66	0.49	1.79	1.89
$\Sigma^2(6)$	0.80	0.55	4.85	3.71
σ_0	0.53	0.50	0.79	0.77
σ_6	0.82	0.65	2.34	1.91
σ_{10}	0.89	0.68	2.85	2.38

*See text for definition of statistics.

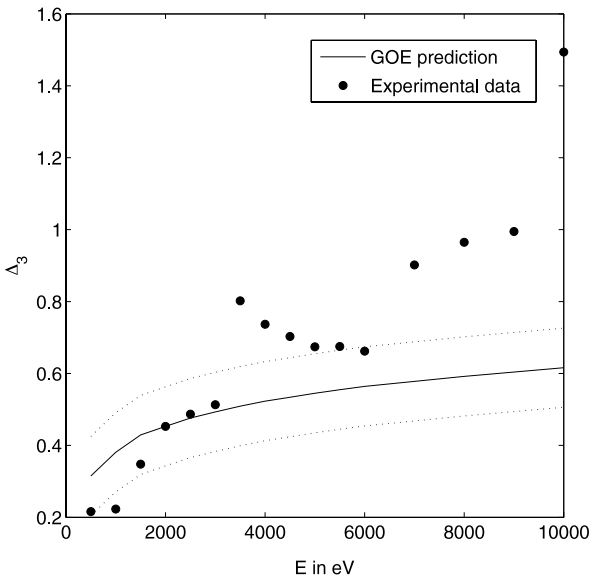

Fig. 3. Analysis of ^{238}U s-wave resonance parameters with the Δ_3 Dyson-Mehta test. X-axis values are the upper boundaries of the energy intervals considered. The straight line is the theoretical GOE prediction, and the dashed line represents the theoretical standard deviation.

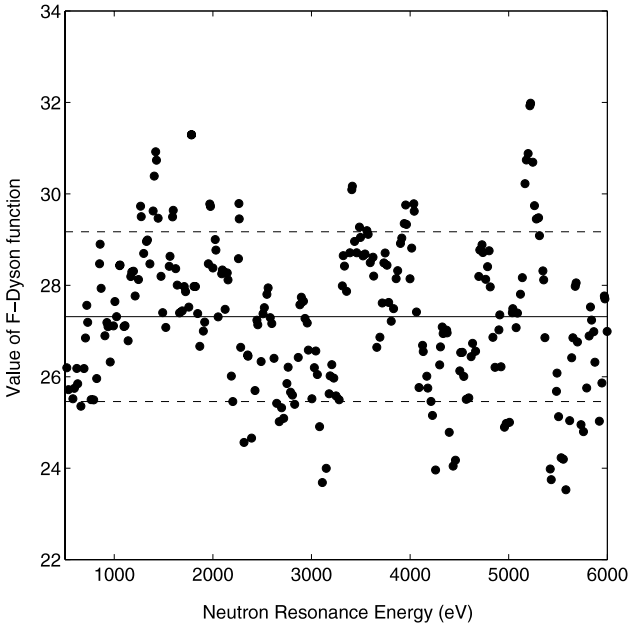

Fig. 4. Analysis of ^{238}U s-wave resonance parameters with the F-Dyson test. The straight line is the theoretical value of the F-Dyson function, and the dashed lines represent the theoretical estimate of the standard deviation (2σ) of the F-Dyson function. Black dots are the experimental values of the F-Dyson function for the ^{238}U s-wave resonance data.

analytical function is computed whose expectation value and standard deviation is known from GOE theory. Local deviation from this theoretical estimate, outside 2σ, can be interpreted as an indication of missed or spurious levels. Figure 4 confirms the possible presence of missed levels around 3 keV, as already indicated by the Δ_3 statistics.

For p-wave resonances, despite the rather good linear behavior of the cumulative number of levels versus energy below 3 keV, all random matrix statistics for $J^\pi = 1/2^-$ or $J^\pi = 3/2^-$ disagree significantly from the GOE prediction, as shown in Table I. The Δ_3 statistic, for instance, is significantly overestimated for $J^\pi = 3/2^-$. This result is not surprising because of the presence in the evaluated set of nonobserved small resonances. Moreover, the spin attribution is experimentally difficult for observed p-wave resonances. Note that RMT gives theoretical results of GOE statistics for mixed and independent spectra; these could permit testing of the entire set of p-wave resonances regardless of the spin.

Table I shows the results of the statistics for individual populations. The conclusion of these tests, based exclusively on resonance energy information, is that the s-wave resonance parameter set seems to be almost pure up to 2.5 keV and the fraction of missing or spurious levels should be small. To support this conclusion, we used a missing-level estimator based on the level-spacing distribution. For a perfect sample, the level-spacing distribution follows the Wigner distribution; however, when a fraction f_m of energy levels is not detected, the theoretical spacing distribution becomes[13]

$$P(D, f_m) = \sum_{k=0}^{\infty} (1 - f_m)^k P(k, r/f_m) \quad . \tag{1}$$

Here, $r = D/D_{obs}$ and $P(k, r)$ is the k-order spacing distribution mentioned in previous sections. For GOE, these distributions were calculated by Monte Carlo or approximated by a Gaussian function with a variance proportional to $\ln(2\pi[k + 1])$. To fit such a distribution and determine f_m, we used the maximum likelihood method, which does not require a binning of the distribution. The most likely value of f_m is obtained by maximizing the likelihood function:

$$L(f_m) = \prod_i P(D_i, f_m) \quad , \tag{2}$$

where D_i are the experimental values of spacings. Applying this estimator, the proportion of missing levels with $J^\pi = 1/2^+$ is found to be $<3\%$ below 5 keV.

To determine the value of average strength function and level spacing, the distribution of evaluated reduced neutron widths, for resonances below 2.5 keV, was fitted with the truncated generalized Porter-Thomas

TABLE II

Average Resonance Parameters from the Statistical Analysis of ^{238}U Resonances

Neutron strength function $l = 0$	$S_0 = (1.03 \pm 0.05)\ 10^{-4}$
Neutron strength function $l = 1$	$S_1 = (1.70 \pm 0.2)\ 10^{-4}$
Average radiative widths $l = 0$	$\Gamma_\gamma = 23.1 \pm 1.0$ meV
Average radiative widths $l = 1$	$\Gamma_\gamma = 21.1 \pm 2.0$ meV
Average spacing $l = 0$	$D_0 = 21.2 \pm 0.2$ eV
Effective scattering radius $l = 0$	$R' = 9.48 \pm 0.05$ fm

distribution $P(\Gamma, \bar{\Gamma}, \nu, \Gamma_t)$ with ν degrees of freedom (small widths below the threshold Γ_t are excluded):

$$P(\Gamma, \bar{\Gamma}, \nu, \Gamma_t)d\Gamma = \begin{cases} 0 & \Gamma < \Gamma_t \\ \dfrac{\nu/2\bar{\Gamma}}{\mathbf{\Gamma}(\nu/2, \nu\Gamma_t/2\bar{\Gamma})}\left(\dfrac{\nu\Gamma}{2\bar{\Gamma}}\right)^{\nu/2-1} & \\ \quad \times \exp\left(-\dfrac{\nu\Gamma}{2\bar{\Gamma}}\right)d\Gamma & \Gamma > \Gamma_t. \end{cases} \tag{3}$$

Here, Γ is the reduced width and $\mathbf{\Gamma}(\nu/2, \nu\Gamma_t/2\bar{\Gamma})$ is the upper incomplete gamma function defined as $\mathbf{\Gamma}(x, y) = \int_y^\infty e^{-t}t^{x-1}\,dt$. In this work, we assume $\nu = 1$ for a single neutron channel. The fitting procedure is again the maximum likelihood method, which consists of determining $\bar{\Gamma}$ by maximizing the likelihood function $L = \prod_i P(\Gamma, \bar{\Gamma}, \nu = 1, \Gamma_t)$. Several threshold values in different energy ranges have been tested to obtain simultaneously the value of $\bar{\Gamma}$ and D. An example of a Porter-Thomas fit for s-wave is shown in Fig. 2. Uncertainty values are given by the maximum likelihood procedure and by the fluctuations of the results with the threshold.

For p-wave resonances, despite significant deviations of experimental statistics from GOE theory, strength functions and average spacings were also estimated. The final results are reported in Table II.

III. EXPERIMENTAL DATABASE

The ^{238}U cross sections above a few kilo-electronvolts have been measured many times in the past. For most of the measurements, detailed information is missing, and sometimes numerical values for experimental data could not be found. Table III presents the selection of measurements used to perform our evaluation.

Below 100 keV, the transmission data measured by Harvey et al.[4] were carefully analyzed. Three samples (thin, medium, and thick) were measured at ORELA using the 200-m flight path. The original data were corrected for resonance shielding effect [i.e, attenuation of energy-averaged transmission in the sample] using a set of artificial but realistic resonance parameters up to 100 keV as input to the SAMMY code.[14] Data from the three samples, averaged over 500-eV bins, give consistent total cross-section values. Above 50 keV, the total cross-section measurement of Poenitz[15] is also a reference measurement and is included in the present analysis. In the common range between the Harvey and the Poenitz data (from 50 to 100 keV), the two experimental cross sections differ by ~2%. Older measurements from Tsubone et al.,[16] Byoun et al.,[17] and Uttley et al.[18] are also included in the fit.

In the capture data measured at ORELA by de Saussure et al.[19] with the ORELAST liquid scintillator tank, the normalization procedure was based on the saturated-resonance technique, using only the first resonance at 6.67 eV. It was assumed that the resonance parameters of this resonance were well known and that the multiple scattering correction was sufficiently accurate.

However, it can be demonstrated that above 100 eV, the de Saussure data need a significant renormalization. As recommended by the recent ORNL analysis below 20 keV, a correction factor of −10% and a background correction of about −50 mb were applied to the original

TABLE III

Experimental Database Used in the Present Evaluation of ^{238}U

Reference	Energy Range (keV)
Total	
Harvey et al. (Ref. 4)	1 to 100
Poenitz et al. (Ref. 15)	49 to 820
Tsubone et al. (Ref. 16)	20 to 930
Byoun et al. (Ref. 17)	12 to 90
Uttley et al. (Ref. 18)	6 to 950
Capture	
Kazakov et al. (Ref. 20)	4 to 460
Moxon et al. (Ref. 21)	1 to 100
de Saussure et al. (Ref. 19)	<100
Macklin et al. (Ref. 5)	0.25 to 100
Inelastic	
Tsang et al. (Ref. 23)	144
Winters et al. (Ref. 24)	82
Barnard et al. (Ref. 25)	75 to 1620
Stromberg et al. (Ref. 26)	95
Moxon et al. (Ref. 27)	68 to 214

data. This normalization procedure gives consistent values with the data of Kazakov et al.,[20] as shown in Fig. 5. The capture data of Moxon[21] were also included in the fit.

The Macklin capture data[5] range from 0.25 to 100 keV. Two uranium samples were measured at ORELA with the ORELAST liquid scintillator tank using the 150-m flight path. The Macklin data were corrected for self-shielding and multiple scattering effects.

The normalization of the capture yields originally used the ^{238}U resonances with small Γ_n, which were assumed to be known with a good accuracy from previous high-resolution transmission experiments by Olsen et al.[22] Thus, the known areas of the resonances in the capture measurements $\Gamma_n\Gamma_\gamma/\Gamma_t \approx \Gamma_n$ could be used to normalize the experimental capture yields. Nevertheless, a rather high uncertainty in the normalization factor is still expected with this technique. The resonance analysis, below 20 keV, suggests a significant upward renormalization by $+15 \pm 5\%$ and a background correction of -110 ± 30 mb for the two samples. However, when these correction factors are applied above 20 keV and after self-shielding and multiple scattering correction, the capture cross sections derived from the two samples are discrepant by more than 10%. For this reason, the Macklin data were not included in the fit. Note that in Ref. 2, the measurement of Macklin (only thin sample data) was used to validate JEF2.2 capture cross section, but the data showed a reasonable agreement only at low energy, below 45 keV and disagreed at higher energy (see Fig. 4 in Ref. 2).

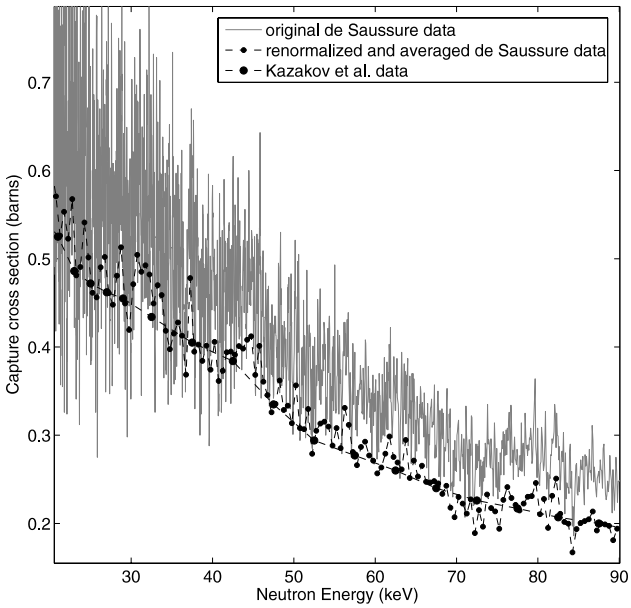

Fig. 5. Comparison between de Saussure capture data for ^{238}U (original data and renormalized data averaged over 1-keV energy bin, as explained in the text) and the Kazakov data.

As in the Fröhner evaluation,[1] the evaluated capture cross section in the present work relies mainly on the Kazakov et al. and Moxon et al. measurements whose normalizations are considered to be more accurate. For inelastic data, measurements taken from the EXFOR database are used.[23–27]

IV. FIT OF AVERAGE CROSS SECTIONS WITH THE STATISTICAL MODEL OF NUCLEAR REACTION

The present SAMMY calculations are based on the statistical theory of nuclear reaction originally developed by Lane and Thomas,[28] Wolfenstein,[29] and Hauser and Feschbach,[30] and extensively studied by Moldauer.[31]

We use the R-matrix form of the collision matrix. After averaging over a large number of resonances, the diagonal elements of the collision matrix $\langle U_{cc}\rangle$ depend on two important parameters: the distant level parameter R_c^∞, which is the real part of the diagonal elements of the average R matrix, and the pole strength s_c, which is the corresponding imaginary part (related to the usual strength function S_c by $s_c = 1/(2ka_c)\sqrt{E/1\text{ eV}}\,S_c$),

$$\langle U_{cc}\rangle = e^{-2i\phi_c}\,\frac{1-(L_c^*-B_c)\langle R_c\rangle}{1-(L_c-B_c)\langle R_c\rangle}$$

$$= e^{-2i\phi_c}\,\frac{1+iP_cR_c^\infty-\pi P_cs_c}{1-iP_cR_c^\infty+\pi P_cs_c}\ , \qquad (4)$$

where

c = neutron channel

$L_c = \hat{S}_c + iP_c$ = vector whose real part is the vector of phase shift $\hat{S}_c$ and the imaginary part is the vector of penetrabilities P_c

ϕ_c = hard-sphere phase shift

$\langle R_c\rangle = R_c^\infty + i\pi s_c$ = diagonal part of the average R matrix

B_c = boundary conditions for the logarithmic derivative of the wave function at the channel radius a_c.

The total cross section is obtained directly from this form of collision matrix. The nonelastic partial cross section is calculated with the Hauser-Feschbach formula using the elastic enhancement and width fluctuation correction factor (WFCF):

$$\sigma_{cc'} = \pi\lambda\!\!\!^{-2}g_c\,\frac{T_cT_{c'}}{\sum_c T_c}\,f_{WFCF}\ . \qquad (5)$$

The transmission coefficients T_c are related to the pole strength, the distant-level parameter, and the penetrabilities. In SAMMY, instead of transmission coefficient, the cross sections (except fission) are expressed as a function of the neutron strength functions S_l and the average radiative widths $\langle\Gamma_\gamma\rangle$. These parameters can be fitted provided that a careful choice of initial value and uncertainties is made. The version 1.0.6 of the SAMMY code (September 2005) was used.

1. The Moldauer prescription[32] was used to compute the WFCF.

2. In the present methodology, the neutron strength functions S_l and distant level parameters R_∞ for the first four partial waves are energy independent in the range 20 to 150 keV and are independent of the spin of the compound nucleus. As shown in Table IV, for $l = 0$ and 1, the initial values of strength functions are taken from the statistical analysis of resonances described in Sec. III and a small uncertainty is given to constrain the fit. S_2 and S_3 are also fitted using S_0 and S_1, respectively, as starting values before the fit.

3. The distant level parameters R_l^∞ are also fitted, but for $l = 0$, the starting value of -0.1255 was adopted with a small uncertainty. This value was deduced from the determination of the effective scattering radius $R'_0 = 9.48$ fm in the resonance analysis using the relationship $R'_0 = a(1 - R_0^\infty)$ valid at low energy for $l = 0$. For higher partial waves, R_l^∞ are fitted using the a priori value of Fröhner[1] and the a priori uncertainty of 10%.

4. The value of average spacing $D_0 = 21.2$ eV (for "zero" neutron energy) is used in the present work and is not fitted. This value renormalizes the level density model at low energy. Note that this value is significantly smaller than the Fröhner determination $D_0 = 23.0$ eV (Ref. 1). The energy dependence of the mean spacing for all values of l and allowed spin J are derived in SAMMY from the composite Gilbert-Cameron formula renormalized to D_0.

5. It was necessary to give a very small uncertainty (0.1 meV) to the average radiative widths Γ_γ to keep realistic adjusted values. A larger uncertainty in the fit leads to an unrealistic low value close to 20 meV. In SAMMY, the energy dependence of the radiative widths is based on the usual giant-dipole resonance model.

6. For inelastic scattering to the first 2^+ level at 45 keV, the direct contribution was included using the optical model parameters and coupled channels calculations of Lopez-Jimenez et al.[33] As shown in Fig. 6, at 150 keV the contribution of the direct inelastic is ~5% of the total inelastic cross section.

The starting and fitted parameters are presented in Table IV. The experimental capture data of Kazakov and Moxon are well reproduced by the present evaluation (see Fig. 7). Quang et al.[34] performed an absolute measurement of the capture cross section at 23 keV. The present value $\sigma_\gamma = 503$ mb is in fairly good agreement with the Quang et al. result $\sigma_\gamma = 491 \pm 11$ mb.

TABLE IV

Values of Initial Parameters and Associated Uncertainties for ^{238}U in the Range 20 to 150 keV*

l	Strength Function $S_l 10^4$	Distant Level Parameter R_l^∞	$\langle\Gamma_\gamma\rangle_l$ (meV)
0	1.030 ± 0.005 **1.042 ± 0.001**	-0.1255 ± 0.005 **-0.1172 ± 0.002**	23.1 ± 0.1 **22.65 ± 0.1**
1	1.700 ± 0.01 **1.893 ± 0.002**	$+0.20 \pm 0.03$ **$+0.1426 \pm 0.008$**	21.1 ± 0.2 **21.26 ± 0.2**
2	1.030 ± 0.05 **1.187 ± 0.004**	-0.20 ± 0.03 **-0.2519 ± 0.02**	$= \Gamma_{\gamma,l=0}$ **22.65**
3	1.700 ± 0.05 **1.490 ± 0.008**	$+0.20 \pm 0.03$ **$+0.1480 \pm 0.03$**	$= \Gamma_{\gamma,l=1}$ **21.26**
Average spacing (low energy) $D_0 = 21.20$ eV			

*Before and after the fit (normal and bold, respectively). Final uncertainties of fitted parameters do not include systematic uncertainties of experimental data and are strongly underestimated.

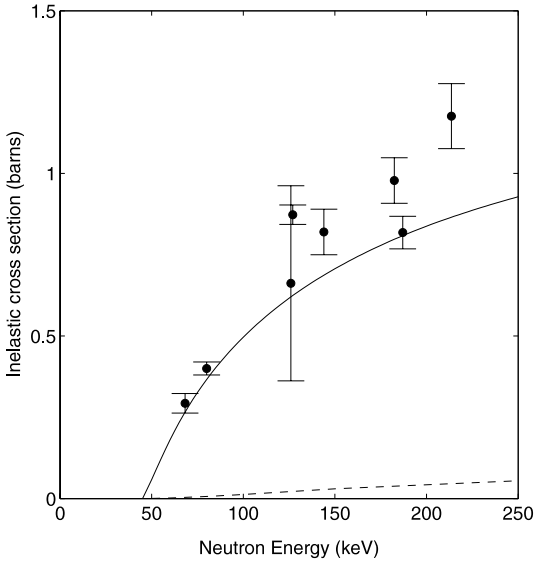

Fig. 6. Comparison of various ^{238}U inelastic experimental data (see the list in Table III) and the present calculation. The dotted line is the contribution of the direct inelastic process.

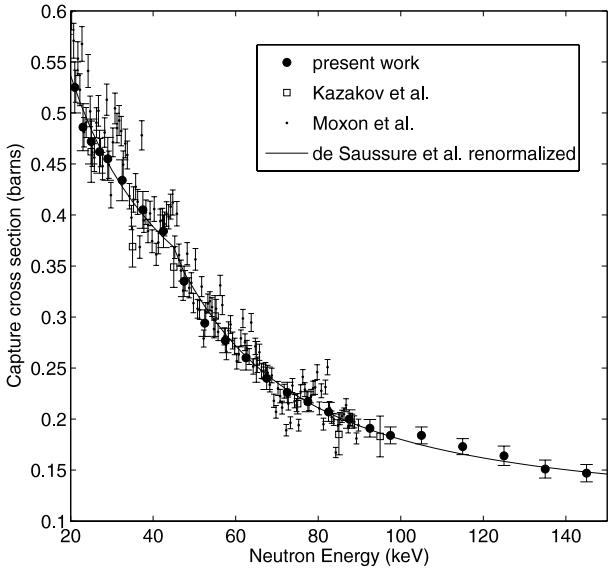

Fig. 7. Comparison of selected ^{238}U capture data with the present evaluation.

As previously noted, a discrepancy of ~2% is observed between the total cross-section values derived from the Harvey and the Poenitz data. The Harvey measurements, displayed in Fig. 8, are considered to be more accurate, and the Poenitz transmission data were consequently renormalized downward by ~2%. We note that above 50 keV, the Poenitz data after renormalization agrees with the Tsubone data[16] (see Fig. 9).

With the present fitted parameters, the experimental total inelastic cross section is fairly well reproduced up to 150 keV, as displayed in Fig. 6. However, at higher energy, experimental data are significantly underestimated. Note that subthreshold fission is not studied in this work.

Figure 10 shows the comparison of the present capture cross section with previous evaluations: Fröhner,[1] Maslov et al.,[35] Carlson,[36] and Lopez-Jimenez et al.[33] adopted in JEFF3.1. The present capture values are very close to the evaluation of Fröhner. Figure 11 presents the comparison of various total cross-section evaluations. As previously explained, above 50 keV, the present total cross-section values are slightly lower than Fröhner and previous works because of the inclusion of Harvey et al. data in the experimental database.

In order to check the present average resonance parameters, total and capture cross sections, averaged over 2-keV energy bins, were computed between 10 and 20 keV using on the one hand, the Reich-Moore formalism associated with resolved resonance parameters from Ref. 3 and on the other hand, the Hauser-Feschbach formalism and the present average resonance parameters. As shown in Table V, a reasonable agreement is obtained for total cross section. The difference is mainly due to the fluctuations of Γ_n distributions in the 2-keV energy bins (each bin contains about 100 resonances). Capture cross section values calculated with resolved resonances are

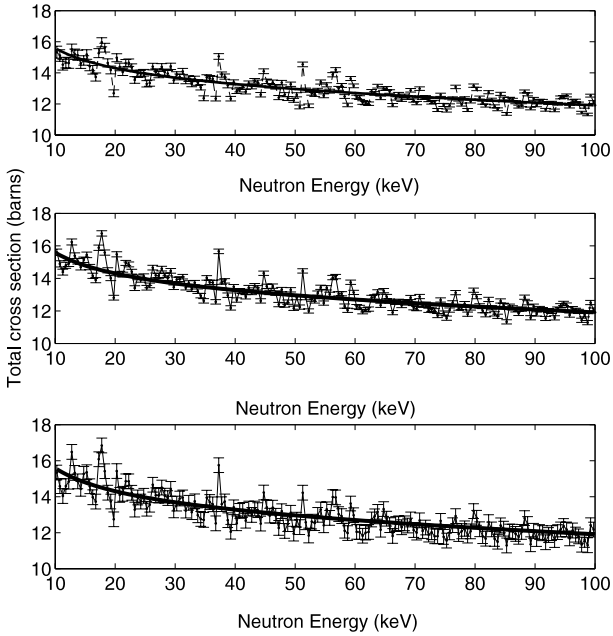

Fig. 8. Comparison of ^{238}U total cross-section experimental data (three samples) from Harvey et al. with the present SAMMY fit.

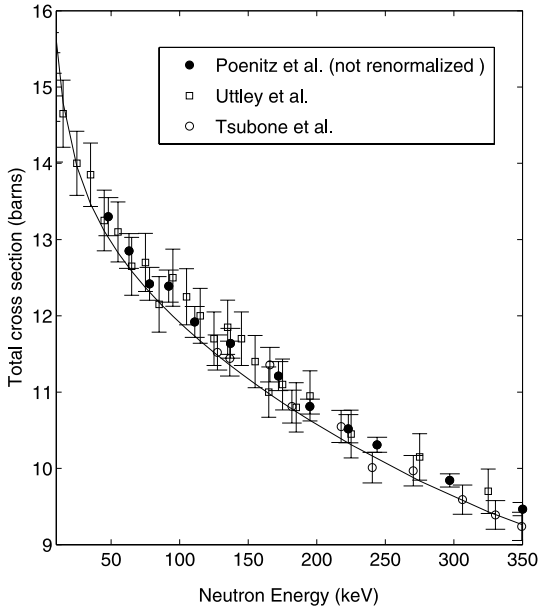

Fig. 9. Comparison of ^{238}U total cross-section experimental data with the present SAMMY fit.

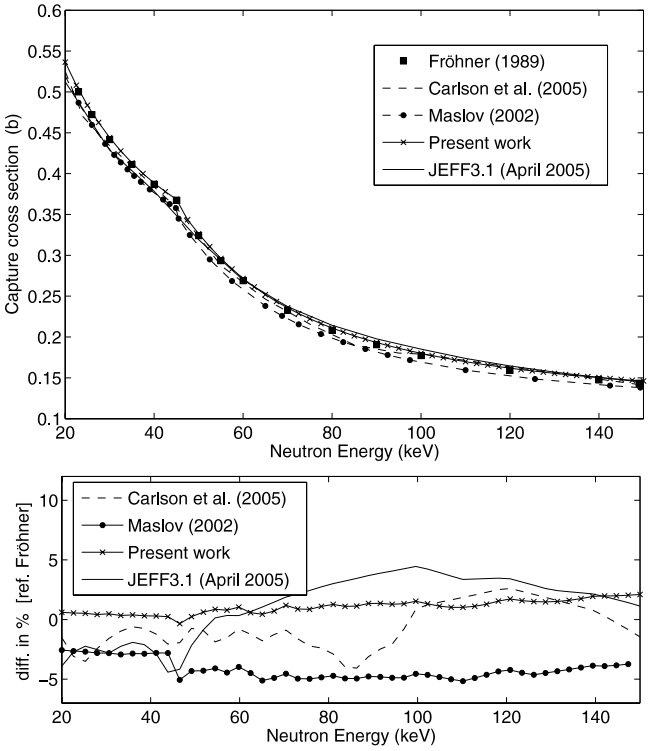

Fig. 10. Comparison of ^{238}U evaluated capture cross sections from previous works with the present SAMMY fit.

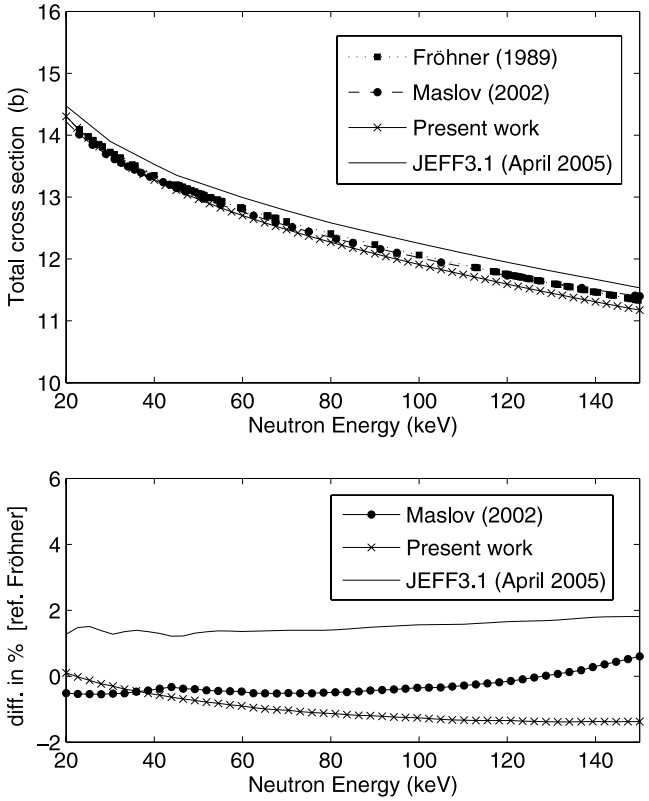

Fig. 11. Comparison of ^{238}U evaluated total cross sections from previous works with the present SAMMY fit.

significantly lower from 5% between 10 and 12 keV, up to 9% in the 19 to 20 keV region. This underestimation might be explained by a significant proportion of missing resonances as well as multiplets in the set of resolved resonance as pointed out in Sec. II.

Given the present experimental database, we estimate the average capture cross section to be known within a 4% accuracy at 20 keV and 10% at 150 keV. The total cross-section uncertainties are estimated to be 3% at 20 keV and 5% at 150 keV. Inelastic data are not known with better than 15% uncertainty. Because this evaluation relies heavily on the Hauser-Feschbach parameterization, a high correlation between average cross-section values at two different energies is expected. Further work is needed to assess rigorously the uncertainties and covariance matrices.

V. ENDF FORMATTING STRATEGY AND REMAINING ISSUES

In the unresolved resonance range, nuclear data users require not only the average cross-section values (tabulated in File 3 of ENDF) but also the information on average resonance parameters to compute some important functionals of the cross section such as transmission $\langle T\rangle_E$, shielding factor $\langle SF\rangle_E$, or self-indication ratios $\langle SI\rangle_E$ that are experimentally measured:

$$\langle T\rangle = \langle e^{-n\sigma_t}\rangle_E \quad , \quad \langle SF\rangle_E = \frac{\langle \sigma\phi\rangle_E}{\langle\sigma\rangle_E\langle\phi\rangle_E} \quad ,$$

$$\langle SI\rangle_E = \frac{\langle e^{-n\sigma_t}\sigma_\gamma\rangle_E}{\langle\sigma_\gamma\rangle_E} \quad . \tag{6}$$

The bracket $\langle\ \rangle_E$ denotes the average over the large number of resonances around the energy E and depends on the temperature and the level of self-shielding, and ϕ is the neutron flux that follows the Boltzmann equation. To calculate these quantities, the ENDF recommends the tabulation of the average resonance parameters versus energy in File 2 as well as the degree of freedom of the corresponding distributions (assuming standard χ-square distributions).

The ENDF-recommended formalism to get the cross section from average resonance parameter is the single-level Breit-Wigner formula averaged over a large number of resonances. This approach is slightly different from the formalism explained in Sec. IV. Only neutron, gamma, and fission channels are allowed. Inelastic

TABLE V

Average Values of Capture and Total Cross Section Computed with the Resolved Resonance Parameters and the Present Average Resonance Parameters*

Energy Range (keV)	Total		Capture	
	Average Cross Section from Resolved Resonance Parameters	Average Cross Section from Average Resonance Parameters	Average Cross Section from Resolved Resonance Parameters	Average Cross Section from Average Resonance Parameters
10 to 12	14.905	15.402	0.6659	0.6989
12 to 14	15.581	15.066	0.6536	0.6504
14 to 16	15.079	14.799	0.5793	0.6111
16 to 18	15.479	14.579	0.5603	0.5781
18 to 20	14.166	14.393	0.5022	0.5498

*Resolved resonance parameters from Ref. 3.

and other channels are lumped into a so-called competitive width, which is used only to calculate total widths and should not be used to compute the corresponding resonant cross section. It is not straightforward to convert the values of average parameters S_l, $\langle\Gamma_\gamma\rangle$, R_l^∞, and $D(l,J)$ used by SAMMY into average resonance parameters because of some differences between SAMMY and ENDF formalisms:

1. The same scattering radius for all partial waves must be used in ENDF instead of an l-dependent distant-level parameter R_l^∞ permitted in SAMMY. Note also that the partial waves $l > 2$ are not allowed by the current ENDF format.

2. The ENDF committee recommends also that the WFCF is calculated with standard averages over the χ-square distribution. This formulation, used in current processing codes such as NJOY (Ref. 37), makes the treatment of temperature and self-shielding effect more convenient with the formalism developed by Hwang.[38] In SAMMY and the modern nuclear model codes, the WFCF can be calculated more accurately using either the Moldauer prescription[39] or an improved formula such as the three-fold integral proposed by Verbaarschot et al.[40]

In the present work, the discrepancies between pointwise cross sections generated by SAMMY and cross sections calculated by NJOY, using only average resonance parameters, are small for the total cross section, <1%. For capture, the discrepancies are small below the first inelastic threshold (<0.7%) but increases at higher energies to reach ≈4% at 140 keV. The traditional way to circumvent these inconsistencies is to use the option LSSF = 1 allowed by the ENDF format that permits the tabulation of the average resonance parameters in File 2 and the average cross-section values in File 3. The File 2 parameters are used only to calculate the shielded cross sections that are normalized with the infinite-dilution values in File 3.

VI. CROSS-SECTION FLUCTUATIONS

One can notice that in the unresolved range, total and capture experimental cross sections, averaged over energy bins <1 keV, exhibit significant fluctuations below 100 keV, which cannot be described by the statistical model. For instance, the two capture measurements of Macklin and de Saussure (after renormalization) show the same structure pattern, and the peaks observed in the total cross section measured by Harvey are clearly correlated with those observed in capture (see Fig. 12).

These fluctuations are explained by the fluctuations of average partial-widths and level-spacing distribution when the number of resonances in the averaging widths is small (this is sometimes called Porter-Thomas fluctuations). Theoretical estimates of the compound cross-section formation variance have been studied.[41–43] Note that an intermediate structure (a nonstatistical effect caused by the presence of special nuclear states like doorway or hallway state) was suspected by Perez et al.[44]

One way to describe fluctuations in evaluated files is to adjust locally the average neutron and gamma widths to reproduce the main structures of the cross section. However, current processing codes for the unresolved resonance range would not be able to cope with this description. Indeed, the analytic approach of Hwang or the usual probability-tables method assumes that the distribution of reduced neutron widths follows a Porter-Thomas distribution. Such a procedure, applied to cross sections with explicit kilo-electron-volt structures, would double-count the fluctuations. For these reasons, Porter-Thomas fluctuations are not described in our evaluation. To our knowledge, the influence of these structures on

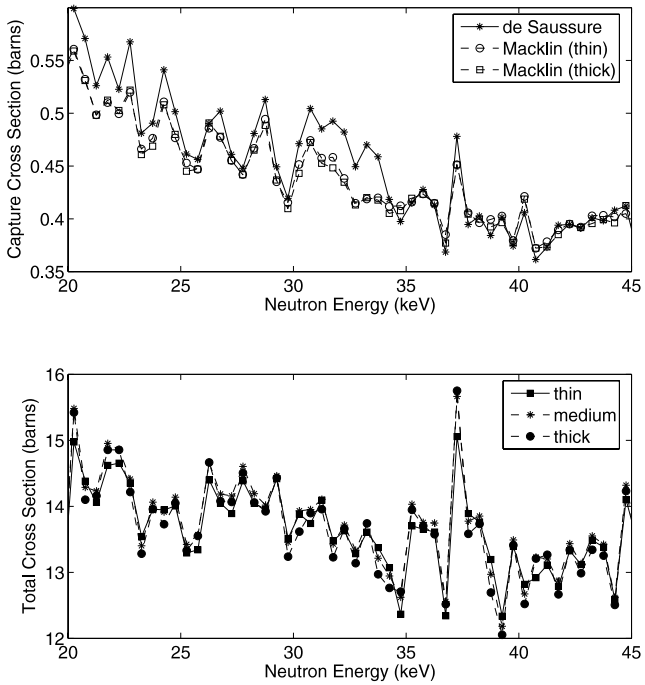

Fig. 12. Average ^{238}U total cross-section data from Harvey et al. (lower figure) and comparison of de Saussure capture data (renormalized data as explained in the text) with the Macklin data for ^{238}U, which are arbitrarily renormalized (upper figure).

self-shielding factors and k_{eff} of fast reactors is still unknown.

VII. CONCLUSION

A new evaluation of the ^{238}U cross sections in the unresolved resonance range, from 20 to 150 keV, is proposed. This evaluation is based on fits of carefully selected measurements, with the statistical model of nuclear reactions of the SAMMY code. Compared to previous works, the present evaluation benefits from the accurate transmission measurements of Harvey et al. up to 100 keV and from a recent evaluation of resolved resonance parameters. The resulting cross sections are not significantly different from Fröhner's evaluation; the main difference is a slightly lower total cross section by 1 to 2% above 50 keV and a different choice of nuclear parameters. This new evaluation has been formatted into an ENDF file (Files 2 and 3) and is available for integral testing. Some aspects of this work merit further investigation:

1. The present ENDF format for average resonance parameters is not fully consistent with modern nuclear statistical models and needs to be revised.

2. A more rigorous approach to get reliable covariance and uncertainty information is needed.

3. Experimental data analyzed in the present work give a good description of the Porter-Thomas fluctuations of the average cross sections in the unresolved resonance range. These structures are not represented in the present work.

4. Experimental validation using thick transmission or self-indication ratio and thermal and fast-reactors benchmarking is also needed.

ACKNOWLEDGMENTS

This work was partly sponsored by CEA and the U.S. Department of Energy Nuclear Criticality Safety Program, under contract DE-AC05-00OR22725 with UT-Battelle, LLC.

REFERENCES

1. F. H. FRÖHNER, "Evaluation of the Unresolved Resonance Range of ^{238}U," *Nucl. Sci. Eng.*, **103**, 119 (1989).

2. F. H. FRÖHNER, "Evaluation of the Unresolved Resonance Range of ^{238}U + *n*, Part II: Differential Data Tests," *Nucl. Sci. Eng.*, **111**, 404 (1992).

3. H. DERRIEN, A. COURCELLE, L. LEAL, N. LARSON, and A. SANTAMARINA, *Proc. Int. Conf. Nuclear Data for Science and Technology,* Santa Fe, New Mexico, September 26–October 4, 2004, American Institute of Physics (2004).

4. J. A. HARVEY et al., *Proc. Int. Conf. Nuclear Data for Science and Technology*, Mito, Japan, May 30–June 3, 1998, Saikon Publishing Co., Tokyo (1988).

5. R. L. MACKLIN et al., *Proc. Int. Conf. Nuclear Data for Science and Technology*, Mito, Japan, May 30–June 3, 1988, Saikon Publishing Co., Tokyo (1988).

6. N. M. LARSON, *Updated Users' Guide for SAMMY: Multilevel R-Matrix Fits to Neutron Data Using Bayes' Equations,* ORNL/TM-9179/R6 and ENDF-364, Oak Ridge National Laboratory (2003).

7. L. M. BOLLINGER and G. E. THOMAS, *Phys. Rev.*, **171**, 6 (1968).

8. F. CORVI, G. ROHR, and H. WEIGMANN, *Proc. Int. Conf. Nuclear Data for Science and Technology,* Mito, Japan, May 30–June 3, 1988, Saikon Publishing Co., Tokyo (1988).

9. C. E. PORTER, *Statistical Theories of Spectra: Fluctuations,* Academic Press, New York (1965).

10. T. A. BRODY et al., *Rev. Mod. Rev.*, **53**, 385 (1981).

11. A. COURCELLE, *Workshop on Perspectives for Nuclear Data for the Next Decade,* Bruyeres-Le-Chatel, France, September 26–28, 2005, Nuclear Energy Agency (2005).

12. H. I. LIOU, H. S. CAMARDA, and F. RAHN, *Phys. Rev. C*, **5**, 3 (1972).

13. O. BOHIGAS and M. P. PATO, *Phys. Lett. B*, **595**, 171 (2004).

14. H. DERRIEN et al., ORNL/TM-2003/291, Oak Ridge National Laboratory (May 2004).

15. W. P. POENITZ, J. F. WHALEN, and A. B. SMITH, "Total Neutron Cross Sections of Heavy Nuclei," *Nucl. Sci. Eng.*, **78**, 333 (1981).

16. I. TSUBONE et al., "Neutron Total Cross Sections of ^{181}Ta and ^{238}U from 24.3 keV to 1 MeV and Average Resonance Parameters," *Nucl. Sci. Eng.*, **88**, 579 (1984).

17. T. Y. BYOUN, R. C. BLOCK, and T. SEMLER, *Proc. Natl. Topl. Mtg. New Developments in Reactor Physics Shielding*, Lake Kiamesha, New York, September 12–15, 1972, U.S. Army Environmental Command (1972).

18. C. A. UTTLEY et al., "Neutron Strength Function Measurements in the Medium and Heavy Nuclei," *Proc. Int. Conf. Nuclear Data for Reactors*, Paris, France, October 17–21, 1966, Vol. 1, p. 165, International Atomic Energy Agency (1966).

19. G. DE SAUSSURE and R. B. PEREZ, "Multilevel Effects in the Unresolved Resonances Region of the Cross Sections of Fissile Nuclides," *Nucl. Sci. Eng.*, **52**, 382 (1973).

20. R. L. E. KAZAKOV et al., *Yad. Konstant.*, **3**, 37 (1986) (in Russian).

21. M. C. MOXON, *Harwell Report,* AERE-R-6074, United Kingdom Atomic Energy Authority (1969).

22. D. K. OLSEN et al., "Measurement and Resonance Analysis of Neutron Transmission Through Uranium-238," *Nucl. Sci. Eng.*, **69**, 202 (1979).

23. F. Y. TSANG and R. M. BRUGGER, "The Differential Neutron Scattering Cross Sections of Uranium-238 at 144 keV," *Nucl. Sci. Eng.*, **65**, 70 (1978).

24. R. R. WINTERS et al., "Uranium-238 Inelastic Neutron Scattering at 82 keV," *Nucl. Sci. Eng.*, **78**, 147 (1981).

25. E. BARNARD et al., *Nucl. Phys.*, **80**, 46 (1966).

26. L. G. STROMBERG and S. SCHWARZ, *Nucl. Phys.*, **71**, 511 (1965).

27. M. C. MOXON et al., *Int. Conf. Nuclear Data for Science and Technology*, Gatlinburg, Tennessee, May 9–13, 1994, American Nuclear Society (1994).

28. A. M. LANE and R. G. THOMAS, *Rev. Mod. Phys.*, **30**, 257 (1958).

29. L. WOLFENSTEIN, *Phys. Rev.*, **82**, 690 (1951).

30. W. HAUSER and H. FESCHBACH, *Phys. Rev.*, **87**, 366 (1952).

31. P. A. MOLDAUER, *Phys. Rev. C*, **11**, 426 (1975).

32. P. A. MOLDAUER, *Nucl. Phys.*, **A344**, 185 (1980).

33. M. J. LOPEZ-JIMENEZ et al., *Proc. Int. Conf. Nuclear Data for Science and Technology,* Santa Fe, New Mexico, September 26–October 4, 2004, American Institute of Physics (2004).

34. E. QUANG and G. KNOLL, "Absolute Measurements of the Fast Neutron Capture Cross Section of ^{238}U," *Nucl. Sci. Eng.*, **110**, 282 (1992).

35. MASLOV et al., *Ann. Nucl. Energy*, **29**, 1707 (2002).

36. A. D. CARLSON, Personal Communication, National Institute of Standards and Technology (2006).

37. R. E. MacFARLANE and D. W. MUIR, LA-12740-M, Los Alamos National Laboratory (Oct. 1974).

38. R. N. HWANG, "Efficient Methods for the Treatment of Resonance Cross Sections," *Nuc. Sci. Eng.*, **52**, 157 (1973).

39. P. A. MOLDAUER, *Phys. Rev. C*, **14**, 764 (1976).

40. J. J. M. VERBAARSCHOT, H. A. WEIDENMULLER, and M. R. ZIRNBAUER, *Phys. Rep.*, **129**, 367 (1985).

41. A. D. CARLSON and H. H. BARSHALL, *Phys. Rev.*, **158**, 4 (1967).

42. F. FRÖHNER, Report NEA/WPEC-15; available at http://www.nea.fr, Nuclear Energy Agency (1994).

43. P. A. EGELSTAFF, *Proc. R. Soc. (London)*, **71**, 910 (1958).

44. R. B. PEREZ, G. DE SAUSSURE, R. L. MACKLIN, and J. HALPERIN, *Phys. Rev. C*, **20**, 528 (1979).